Published August 22, 2019

Original Research

Core Ideas

- Macropore flow may be enhanced in partly frozen soil.
- We developed a dual-permeability modeling approach for frozen soils.
- Four test cases of increasing complexity were evaluated.
- Modeling results are in agreement with current process understanding.
- Measured data are lacking for a more quantitative evaluation of the model.

A Dual-Permeability Approach for Modeling Soil Water Flow and Heat Transport during Freezing and Thawing

Mats Larsbo,* Roger Holten, Marianne Stenrød, Ole Martin Eklo, and Nicholas Jarvis

Preferential flow may become significant in partially frozen soils because infiltration can occur through large, initially air-filled pores surrounded by a soil matrix with limited infiltration capacity. The objectives of this study were to develop and evaluate a dual-permeability approach for simulating water flow and heat transport in macroporous soils undergoing freezing and thawing. This was achieved by introducing physically based equations for soil freezing and thawing into the dual-permeability model MACRO. Richards' equation and the heat flow equation were loosely coupled using the generalized Clapeyron equation for the soil micropore domain. Freezing and thawing of macropore water is governed by a first-order equation for energy transfer between the micropore and macropore domains. We assumed that macropore water was unaffected by capillary forces, so that water in macropores freezes at 0°C. The performance of the model was evaluated for four test cases: (i) redistribution of water in the micropore domain during freezing, (ii) a comparison between the first-order energy transfer approach and the heat conduction equation, (iii) infiltration and water flow in frozen soil with an initially air-filled macropore domain, and (iv) thawing from the soil surface during constant-rate rainfall. Results show that the model behaves in accordance with the current understanding of water flow and heat transport in frozen macroporous soil. To improve modeling of water and heat flow in frozen soils, attention should now be focused on providing experimental data suitable for evaluating models that account for macropore flow.

Abbreviations: FOET, first-order energy transfer.

M. Larsbo (ORCiD iD 0000-0002-5162-2323) and N. Jarvis, Dep. of Soil and Environment, Swedish Univ. of Agricultural Sciences (SLU), P.O. Box 7014 75007, Uppsala, Sweden; R. Holten, M. Stenrød and O.M. Eklo, Dep. of Pesticides and Natural Products Chemistry, Division of Biotechnology and Plant Health, Norwegian Institute of Bioeconomy Research (NIBIO), P.O. Box 115, NO-1431 Ås, Norway; R. Holten and O.M. Eklo, Dep. of Plant Sciences, Faculty of Bio Sciences, Norwegian Univ. of Life Sciences, P.O. Box 5003, N-1432 Ås, Norway. *Corresponding author (Mats.Larsbo@slu.se).

Received 30 Jan. 2019.
Accepted 20 June 2019.
Supplemental material online.

Citation: Larsbo, M., R. Holten, M. Stenrød, O.M. Eklo, and N. Jarvis. 2019. A dual-permeability approach for modeling soil water flow and heat transport during freezing and thawing. Vadose Zone J. 18:190012. doi:10.2136/vzj2019.01.0012

Freezing and thawing strongly affects water flow in soil since ice may block a large part of the pore space, thereby preventing infiltration. At a larger scale, the reduced permeability of frozen soil layers influences the partitioning of precipitation between surface runoff into rivers and lakes and infiltration into the soil that may replenish groundwater storage (e.g., Ireson et al., 2013; Lundberg et al., 2016). The effects of freezing on soil hydrology are often most significant during snowmelt, when large amounts of water may reach the soil surface in a short amount of time.

Preferential flow in soil macropores has long been recognized as an important process that influences vadose zone hydrology from the pore scale to the hillslope scale (Beven and Germann, 1982; Jones, 2010; Jarvis et al., 2016). Preferential flow may become even more significant under frozen conditions when infiltration occurs through large, initially air-filled pores surrounded by a soil matrix with limited infiltration capacity (e.g., Kane, 1980; Stadler et al., 2000, Mohammed et al., 2018). Despite its relevance in temperate and sub-polar climate zones, preferential flow in frozen soils has, to date, received little attention. Some noteworthy exceptions are the studies by van der Kamp et al. (2003) and Watanabe and Kugisaki (2017). Van der Kamp et al. (2003) demonstrated the importance of macropores for frozen soil infiltration rates in the Canadian prairies using single-ring infiltrometers. They showed that infiltration rates were smaller for cultivated soils with few macropores than for permanent grassland soils containing well-developed macropore networks. During snowmelt, the unsaturated large macropores in the grassland soil still

had substantial infiltration capacities, generally exceeding the maximum probable rate of snowmelt. The effects of macropores on water flow through frozen soil have recently also been demonstrated in column-scale laboratory experiments. Watanabe and Kugisaki (2017) studied water flow through initially air-filled artificially created vertical macropores of different sizes. The exchange of energy between the frozen soil matrix and the water in the macropores resulted in freezing of the infiltrating water for macropores with a diameter of 2 mm. However, for a setup with 5-mm-diameter vertical pores, the water flow rate was high enough to limit freezing of the infiltrating water, resulting in a fast drainage response at the bottom of the column.

A number of numerical models of water flow through soil that account for the effects of freezing and thawing have been developed since the 1970s. Many of these models account for freezing by coupling Richards' equation for water flow and the heat flow equation using the generalized Clapeyron equation, which relates the capillary pressure to temperature during phase change. Such physically based modeling approaches were recently reviewed by Kurylyk and Watanabe (2013) and Mohammed et al. (2018). As far as we know, the only model that addresses the important effect of macropores on water flow and heat transport is the model by Stähli et al. (1996), which is included in the COUP model (Jansson, 2012). They developed a modeling concept that accounted for the fact that soils often freeze when the soil is unsaturated. They argued that under such conditions, the water in the smallest pores will remain unfrozen, the water in intermediate sized pores will be frozen, and the largest pores will be air filled. If the largest pores remain air filled during winter, they will contribute to the infiltration capacity of the soil during spring snowmelt. In their model, although they make no distinction between soil macropores and the soil matrix, water infiltrating into the large (initially) air-filled pores constitutes a high-water-flow domain. As water flows through the high-flow domain, it may freeze due to heat transfer from the high-flow domain to the low-flow domain, resulting in a reduction of the volume of water in the high-flow domain and a shift in the boundary between the low-flow domain and the ice domain toward larger pores. This approach was shown to improve simulation results for the onset of drainage during snowmelt (Stähli et al., 1996).

Based on their review on infiltration and macropore flow in frozen soils, Mohammed et al. (2018) proposed a "matrix–macropore conceptual framework for water and heat transfer in unsaturated frozen soil." This conceptual model includes a fixed distinction between the micropore and macropore domains based on a pore size threshold. Such a distinction between pore domains has, since the 1990s, been used in dual-permeability models to model preferential water flow in macroporous soil, albeit without accounting for freezing (e.g., Jarvis et al., 1991; Gerke and van Genuchten, 1993). These models account for nonequilibrium in pressure potentials between the soil matrix and larger pores, which is often encountered in soils. For frozen soils, this approach would distinguish larger, air-filled micropores, which can be blocked by ice due to redistribution of water during freezing, from macropores that generally remain open during soil freezing and can only be blocked due to freezing of infiltrating water (Mohammed et al., 2018). As far as we know, there are no numerical simulation models available that can account for the effects of freezing on preferential water flow through macropores using a dual-permeability approach.

The objectives of this study were to develop and evaluate a dual-permeability approach for water flow and heat transport in macroporous soils undergoing freezing and thawing. This was achieved by introducing physically based equations for soil freezing and thawing into the MACRO model (Larsbo et al., 2005). We tested the model for water flow in the micropore domain against available measured data on the redistribution of water during freezing. Illustrative scenario simulations were also performed to demonstrate the effects of soil macropores on water flow and heat transport in partially frozen soils.

Materials and Methods

The MACRO Model

MACRO is a one-dimensional dual-permeability model of variably saturated water flow and reactive solute transport in soil (Larsbo et al., 2005; Jarvis and Larsbo, 2012). It has been used since the early 1990s as a research tool to investigate the effects of macropore flow on soil hydrology and contaminant transport under transient field conditions and is one of the models used in risk assessments for pesticide leaching in the European Union (FOCUS Working Group on Surface Water Scenarios, 2001). Here we give a very brief description of the processes that are most relevant for the further development of approaches for water flow and heat transport under winter conditions.

Rain or snowmelt is partitioned into infiltration into micropores and macropores assuming that water will only infiltrate into macropores when the infiltration capacity of the micropore domain is exceeded. Water flow in micropores is calculated with Richards' equation using soil hydraulic properties described by the Mualem–van Genuchten model (Mualem, 1976; van Genuchten, 1980). A modified kinematic wave equation is used to calculate water flow in soil macropores, q_{mac} (mm h^{-1}):

$$q_{mac} = K_{mac,sat} S_{mac}^{n^*} \quad [1]$$

where the subscript *mac* denotes the macropore domain, $K_{mac,sat}$ (m s^{-1}) is the saturated macropore hydraulic conductivity, n^* (dimensionless) is the kinematic exponent, and $S_{mac} = \theta_{mac}/\varepsilon_{mac}$ (dimensionless) is the degree of saturation, where θ_{mac} (m^3 m^{-3}) is the volumetric water content and ε_{mac} (m^3 m^{-3}) is macroporosity.

First-order water exchange from macropores to the micropore domain, S_w (s^{-1}), is calculated as

$$S_w = \frac{G_f D_w S_{mac} \gamma_w}{d^2} (\theta_b - \theta_{mic}) \quad [2]$$

where G_f (dimensionless) is a geometry factor (set internally to 3 for a rectangular slab geometry; Gerke and van Genuchten, 1996),

D_w (m^2 s^{-1}) is the soil water diffusivity, γ_w (dimensionless) is a scaling factor (Jarvis, 1994), d (m) is the diffusion path length (a parameter related to the geometry of the pore network), and θ_b (m^3 m^{-3}) and θ_{mic} (m^3 m^{-3}) are the saturated and actual water contents in the micropore domain, respectively.

In previous versions of the MACRO model, soil temperatures were calculated with a heat conduction equation assuming equilibrium between pore domains and without considering freezing–thawing.

A Dual-Permeability Approach for Coupled Water Flow and Heat Transport Accounting for Soil Freezing

Water flow in macropores is often fast, and residence times in a frozen soil layer may be short compared with the time it would take to freeze the macropore water (Watanabe and Kugisaki, 2017; Mohammed et al., 2018). Under such conditions, the assumptions of equilibrium in temperature between pore domains is not valid. In the following, we describe a dual-permeability approach for water flow and heat transport in soil that accounts for the nonequilibrium in both water pressures and temperatures that often occurs in soil during freezing and thawing. Depending on the temperature, water in the micropore and macropore domains may exist both in liquid form and as ice.

The porosity in the micropore domain is given by

$$\varepsilon_{mic,tot} = \theta_{mic,liq} + \theta_{mic,ice} + a_{mic} \quad [3]$$

where the subscript *mic* denotes the micropore domain, $\theta_{mic,liq}$ (m^3 m^{-3}) and $\theta_{mic,ice}$ (m^3 m^{-3}) are the volumetric liquid water and ice contents (assuming no change in density), respectively, and a_{mic} (m^3 m^{-3}) is the volumetric air content. A similar equation can be written for the macropores. To denote the macropore domain we use the subscript *mac*. The dual-permeability approach for partly frozen soil is illustrated in Fig. 1. With this new approach, preferential water flow in soil macropores in partly frozen soil may take place both when the soil matrix is saturated and when it is unsaturated. For the case with water flow in macropores bypassing an unsaturated matrix (i.e., nonequilibrium flow), water will be transferred from the macropores to the soil matrix according to Eq. [2]. For the case with a saturated matrix, the approach has similarities to the model by Stähli et al. (1996) although the hydraulic functions used are different between the models. Although not the focus in this study, preferential flow frequently occurs also when the soil is unfrozen. As far as we know, the MACRO model, including the new approach presented in this study, is the only model that handles preferential flow for both unfrozen and frozen conditions. Furthermore, although the effects of freezing on solute transport have not been implemented in the model, MACRO also accounts for nonequilibrium conditions in solute concentrations (Larsbo et al., 2005), which would in principle enable future simulation of preferential transport of solutes in frozen soil, even when the matrix is fully saturated.

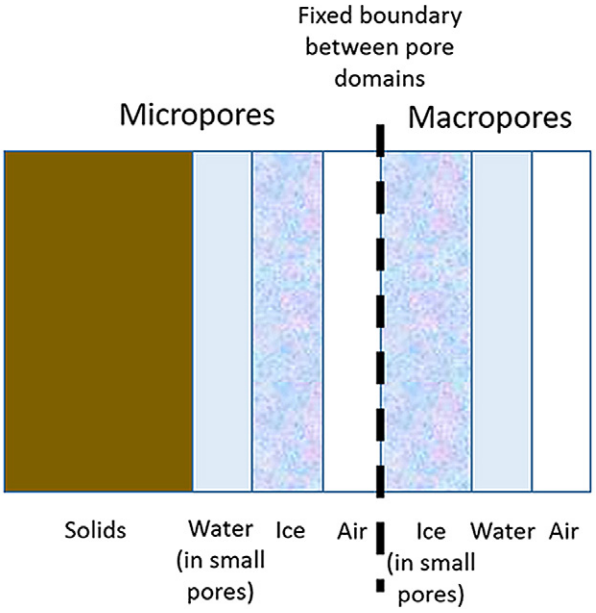

Fig. 1. Schematic illustration of the dual-permeability approach for partly frozen soil.

Micropore Domain Approaches

For the micropore domain, we followed the physically based approach for combining Richards' equation and the heat flow equation (accounting for conduction, convection, and latent heat transfer) given by Hansson et al. (2004), with the exception that we did not include vapor flow. We used an analogy between freezing and drying to account for the effects of ice on water flow (Koopmans and Miller, 1966). This means that water flow is driven by gradients in pressure potentials corresponding to the liquid water content. The hydraulic conductivity of soils is drastically reduced in frozen soils (Kane, 1980; Seyfried and Murdock, 1997). This is naturally handled by the decrease in liquid water contents during freezing. However, to further reduce the hydraulic conductivity in frozen soils, $K_{mic,frozen}$ (m s^{-1}), we also included an empirical impedance factor, Ω (dimensionless), in accordance with Hansson et al. (2004):

$$K_{mic,frozen} = 10^{-\Omega Q} K_{mic,unfrozen} \quad [4]$$

where $Q = \theta_{mic,ice}/(\theta_{mic,liq} + \theta_{mic,ice})$ and $K_{mic,unfrozen}$ (m s^{-1}) is the hydraulic conductivity calculated from the Mualem–van Genuchten model. The impedance factor was included to limit water flow toward the freezing front (Lundin, 1990), although the physical basis for doing so is not clear (Kurylyk and Watanabe, 2013).

Soil temperatures were modeled using the one-dimensional (vertical) heat flow equation:

$$\frac{\partial C_{mic,tot} T_{mic}}{\partial t} - L_f \rho_{ice} \frac{\partial \theta_{mic,ice}}{\partial t} = \frac{\partial}{\partial z}\left[k_h \frac{\partial T_{mic}}{\partial z}\right] - C_{liq} \frac{\partial q_{mic} T_{mic}}{\partial z} - (EX_{cond} + EX_{conv}) \quad [5]$$

where $C_{mic,tot}$ (J m^{-3} K^{-1}) is the soil heat capacity of the soil micropore domain, T_{mic} (K) is temperature, k_h (W m^{-1} K^{-1}) is the thermal conductivity, C_{liq} (J m^{-3} K^{-1}) is the heat capacity of water, q_{mic} (m s^{-1}) is the water flow rate, L_f (J kg^{-1}) is the latent heat of freezing, ρ_{liq} (Mg m^{-3}) is the density of ice, and EX_{cond} and EX_{conv} (W m^{-3}) are the conductive and convective energy exchanges with the macropore domain, respectively. Finally, t (s) is time and z (m) is the vertical coordinate.

To solve Eq. [5], the two terms on the left-hand side were combined according to Hansson et al. (2004) to achieve an expression for the apparent volumetric heat capacity, which accounts for the latent heat of freezing. We used the generalized Clapeyron equation to combine Richards' equation with the heat flow equation by introducing the hydraulic capacity, $C = \partial\theta_{mic}/\partial h_{mic}$ (m^{-1}), where h (m) is the pressure head, in the expression for the apparent heat capacity. The Crank–Nicholson numerical scheme used in previous versions of the MACRO model was extended to include the apparent heat capacity term, convection of heat, and conductive and convective exchanges between pore domains.

It is challenging to solve Richards' equation numerically for near-saturated and saturated conditions when accounting for freezing and thawing due to the large gradients in pressure potential that occur at the freezing–thawing front. For example, as a result, the freezing and thawing module of HYDRUS-1D runs only for unsaturated conditions (Šimůnek et al., 2016). Here, to handle these difficulties we used the geometric mean [$K_{geo\ mean,i+1/2} = \sqrt{(K_{mic,frozen,i} K_{mic,frozen,i+1})}$ where i denotes the numerical layer] of hydraulic conductivities or the minimum hydraulic conductivity to calculate water fluxes instead of the arithmetic mean, which is otherwise used in the MACRO model. The use of geometric means or minimum hydraulic conductivities gives more weight to layers with small conductivities and thereby reduces flow at the boundaries between frozen and unfrozen numerical layers.

Soil thermal properties are affected by the presence of ice in the pore system. The soil heat capacity of the soil micropore domain accounting for the contribution of ice is given by the sum of the heat capacities of the mineral phase, the water phase, and the ice phase according to

$$C_{mic,tot} = C_{solids}\left(1-\varepsilon_{mic,tot}\right) + C_{liq}\theta_{mic,liq} + C_{ice}\theta_{mic,ice} \quad [6]$$

where C_{water} = 4.2 MJ m^{-3} K^{-1} and C_{ice} = 1.9 MJ m^{-3} K^{-1} are the heat capacities of liquid water and ice, respectively, while C_{solid} (MJ m^{-3} K^{-1}) is the heat capacity of the solid phase (except ice) given by

$$C_{solids} = C_{om} f_{om} + C_{mineral}\left(1-f_{om}\right) \quad [7]$$

where C_{om} = 2.7 MJ m^{-3} K^{-1} and $C_{mineral}$ = 2.0 MJ m^{-3} K^{-1} are the heat capacities of organic matter and mineral soil, respectively, and f_{om} (dimensionless) is the fraction of organic matter.

Thermal conductivity, k_h (W m^{-1} K^{-1}) was estimated using the modified form of the model proposed by Campbell (1985) and given by Hansson et al. (2004):

$$k_h = C_1 + C_2\left(\theta_{liq} + F\theta_{ice}\right) - \left(C_1 - C_4\right)\exp\left\{-\left[C_3\left(\theta_{liq} + F\theta_{ice}\right)\right]^{C_5}\right\} \quad [8]$$

where $F = 1 + F_1\theta_{ice}^{F2}$. The constants C_1 to C_5, F_1, and F_2 can be estimated by fitting Eq. [8] to measured data.

Macropore Domain Approaches

In analogy with the assumption of gravity-driven water flow in the macropore domain, the freezing temperature is assumed to be unaffected by capillary forces (i.e., liquid water and ice can only exist simultaneously at T_{mac} = 0°C). We did not account for conductive heat transport in the macropores, where water flow velocities usually are large. Temperatures in macropore water are, hence, only influenced by vertical convection of energy and lateral energy exchange between the pore domains. This means that thawing of water in a completely frozen saturated macropore where all the water is immobile is governed solely by energy exchange between the pore domains.

The heat flow equation for the macropores is given by

$$\frac{\partial C_{mac,tot} T_{mac}}{dt} - L_f\rho_i\left(\frac{\partial\theta_{mac,ice}}{\partial t}\right) = -C_{liq}\frac{\partial q_{mac} T_{mac}}{\partial z} + \left(EX_{cond} + EX_{conv}\right) \quad [9]$$

where the terms on the left-hand side represent changes in the energy content given by the temperature of the macropore water and changes in the latent heat content, respectively, the terms on the right-hand side represent convection of sensible heat with flowing water and heat exchange between the pore domains, $C_{mac,tot}$ (J m^{-3} °C^{-1}) is the volumetric heat capacity for the macropore domain (accounting for both liquid water and ice), and q_{mac} (m s^{-1}) is the water flow in the macropores. Since liquid water and ice can only exist simultaneously at T_{mac} = 0°C, it is straightforward to solve Eq. [9] from the known energy inputs to a numerical layer (see the Supplemental Material).

From the assumption that freezing in macropores is unaffected by capillary forces, it follows that the smallest water-filled macropores will freeze first (Fig. 1) because water flow rates are comparably small and the contact area between the micropore domain and the water in macropores is large in relation to the water volumes. This leads to a simple equation for the unsaturated hydraulic conductivity in partly frozen macropores (m s^{-1}):

$$K_{mac,frozen} = K_{mac,sat}\left(\frac{\theta_{mac,tot}}{\varepsilon_{mac}}\right)^{n^*} - K_{mac,sat}\left(\frac{\theta_{mac,ice}}{\varepsilon_{mac}}\right)^{n^*} \quad [10]$$

where $\theta_{mac,tot} = \theta_{mac,liq} + \theta_{mac,ice}$ is the total water content in the macropore domain.

Exchange between Pore Domains

The first-order mass transfer approach has been shown to work well for the exchange of water and solutes between pore domains (Gerke and van Genuchten, 1993, 1996). Here we use a similar approach for the first-order energy transfer (FOET)

between pore domains, EX_{cond} (J s^{-1} m^{-3}), with differences in temperature as the driver:

$$EX_{cond} = \frac{G_f S_{mac,tot} k_h}{d^2}(T_{mic} - T_{mac}) \quad [11]$$

where G_f (dimensionless) is a geometry factor, $S_{mac,tot}$ (dimensionless) is the degree of saturation in the macropore domain, including both water and ice, which accounts for the contact surface area between the water in the macropores and the soil micropore domain, and d (m) is the diffusion path length.

The convective exchange term, EX_{conv} (J s^{-1} m^{-3}) is given by

$$EX_{conv} = S_w (T_{mic/mac} C_{liq}) \quad [12]$$

where $T_{mic/mac}$ (°C) is the temperature in the micropore domain or macropore domain depending on the direction of S_w.

Test Cases

Redistribution of Water in the Micropore Domain during Freezing (Test Case 1)

Large gradients in pressure potential may develop when water freezes. Despite the limited permeability, this may lead to a significant redistribution of water from unfrozen soil toward the freezing front (e.g., Williams and Smith, 1989; Stähli et al., 1999). To evaluate the numerical implementation of the model for the micropore domain, we used the data on water redistribution during freezing from Mizoguchi (1990). The data were extracted from Hansson et al. (2004) using WebPlotDigitizer Version 3.12. This dataset has become a standard for benchmarking physically based models of water flow during freezing (e.g., Hansson et al., 2004; Dall'Amico et al., 2011; Kelleners, 2013).

A 20-cm-high soil column (Kanagawa sandy loam) was frozen from the top using a circulating fluid with a temperature of −6°C. Heat transport through the soil surface, $q_{h,surf}$ (W m^{-2}), was modeled using a variable heat flow boundary condition:

$$q_{h,surf} = -h_c (T_{top} - T_{coolant}) \quad [13]$$

where h_c (W m^{-2} K^{-1}) is a heat transfer coefficient and T_{top} (K) and $T_{coolant}$ (K) are the temperatures of the soil surface and of the cooling fluid, respectively. The initial water contents ($\theta_{initial}$ = 0.33 m^3 m^{-3}) and temperatures ($T_{initial}$ = 6.7°C) were constant with depth.

We parameterized the model according to Hansson et al. (2004). The van Genuchten parameters were: saturated water content θ_s = 0.535 m^3 m^{-3}, residual water content θ_r = 0.05 m^3 m^{-3}, and shape parameters α = 0.0111 cm^{-1} and n = 1.48. The saturated hydraulic conductivity of the micropore domain (K_{sm} = 2.66 mm h^{-1}) was calculated from the measured total saturated hydraulic conductivity of 11.5 mm h^{-1} and a pressure potential defining the boundary between pore domains set to −10 cm as suggested by Jarvis (2007). The hydraulic conductivity was adjusted using an impedance factor, Ω (dimensionless), set to 7 (Eq. [4]). The parameter values of the model used to calculate thermal conductivity (Eq. [8]) were: C_1 = 0.55 W m^{-1} K^{-1}, C_2 = 0.80 W m^{-1} K^{-1}, C_3 = 3.07, C_4 = 0.13 W m^{-1} K^{-1}, C_5 = 4, F_1 = 13.05, and F_2 = 1.06. Finally, h_c and $T_{coolant}$ were set to 28 W m^{-2} K^{-1} and −6°C.

None of the models that have previously been compared with the Mizoguchi dataset are identical to our model. For comparison, we also included modeling results from Dall'Amico et al. (2011), again extracted using WebPlotDigitizer Version 3.12. Dall'Amico et al. (2011) used a different model for estimating the thermal conductivity and different numerical methods (including the spatial and temporal discretization).

Comparison between First-Order Energy Transfer and the Heat Flow Equation (Test Case 2)

To illustrate the FOET approach, we simulated thawing of an initially frozen soil micropore domain through lateral energy transfer from a saturated macropore domain with a constant temperature, T_{mac} (Fig. 2). We used the same thermal properties as for Test Case 1. Simulation results for the FOET approach were compared with results from a numerical solution of the

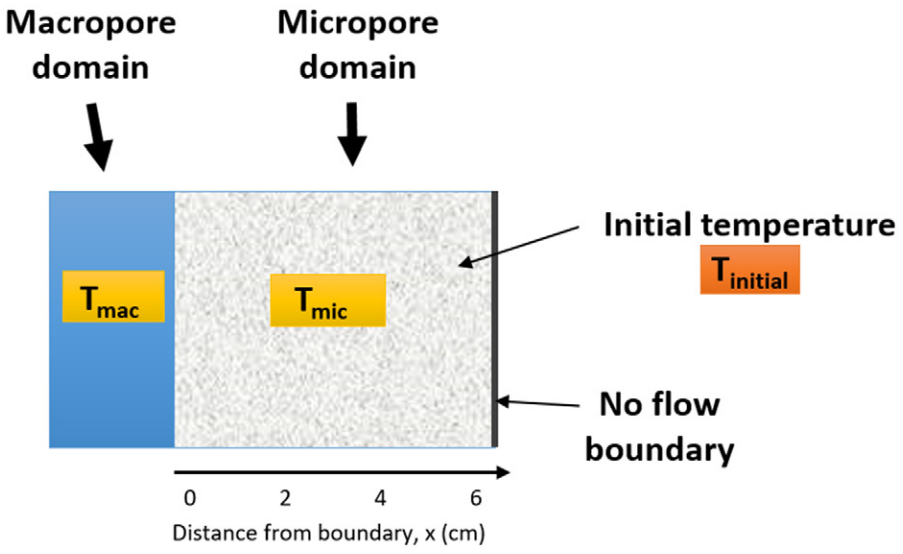

Fig. 2. The simulation domain for the comparison between the first-order energy transfer approach and the one-dimensional (1D) heat conduction equation. The boundary temperature is constant at T_{mac}. For the 1D heat flow equation, T_{mic} is a function of the distance from the boundary between pore domains, x (cm).

one-dimensional heat conduction equation (Eq. [5] assuming no convective heat transport and no exchange between the micropore and macropore domains). For the FOET approach, the temperature in the micropore domain, T_{mic}, is defined by one single value at each time step. For the heat flow equation, the temperature in the micropore domain will vary with distance from the boundary, x (m). For this case, arithmetic mean values were calculated and used in the comparisons.

The boundary conditions for the heat conduction equation were given by:

$$T_{mic}(t, x = 0) = T_{mac} \quad [14]$$

$$q_h(t, x = d) = 0 \quad [15]$$

where q_h (W m^{-1} K^{-1}) is the heat transport in the simulated soil aggregate and d (m) is the diffusion path length, which for this test case was set to 60 mm.

The initial condition was given by

$$T_{mic}(t = 0, x) = T_{initial} \quad [16]$$

where $T_{initial}$ (°C) is the initial temperature.

Simulations were run with and without soil freezing with T_{mac} set to 5°C and $T_{initial}$ set to −5°C. The heat flow equation was solved using the Crank–Nicholson numerical scheme used to solve Eq. [5]. The FOET approach was solved with an explicit Euler method in R (R Core Team, 2018). For the simulations without freezing, heat capacities and thermal conductivities are constant, while they vary with ice content for the simulations accounting for freezing.

Infiltration into Frozen Soil during Controlled Irrigation with Initially Air-Filled Macropores (Test Case 3)

There are currently no suitable data available in the literature for a quantitative evaluation of the modeling approach used for the macropore domain. To illustrate the behavior of the macropore model, we simulated freezing of water infiltrating into initially air-filled macropores. For these simulations, no water flow or heat transport was allowed in the micropore domain, which was saturated and kept at a constant temperature of −2°C. The soil was irrigated for 6 min every 30 min at a rate of 1 mm h^{-1}. In total, seven irrigations were simulated. The irrigation water had a temperature of 1°C. Because no water flow occurred in the micropore domain, all irrigation water was directed to the macropore domain. The macroporosity was 0.015 m^3 m^{-3}, the macropore saturated hydraulic conductivity was 2 mm h^{-1}, and the kinematic exponent was 2 (dimensionless). This means that at saturation the water velocity was 133 mm h^{-1}. Freezing of infiltrating water in the macropores was, for this case, governed only by the conductive energy exchange between pore domains (Eq. [9] without convective exchange). The diffusion path length, d, was set to 60 mm (Eq. [11]) to represent soils with intermediate potential for nonequilibrium flow (i.e., the conductive exchange of energy between pore domains was intermediate).

Thawing of Initially Frozen Soil during Constant Rainfall (Test Case 4)

To evaluate the complete model, we simulated thawing from the soil surface of an initially frozen (T = −2°C) 20-cm-high soil column during constant rainfall at 1.5 mm h^{-1}. The initial total water contents (liquid water and ice) were calculated from drainage equilibrium with a water table at the bottom of the column. The conductive heat transport at the top boundary was calculated from an air temperature set to 7°C, while the conductive heat transport at the bottom boundary was set to zero. We divided the soil column into 80 equally thick numerical layers. As in Test Case 1, we parameterized the micropore domain according to Hansson et al. (2004). The macroporosity was set to 0.015 m^3 m^{-3}, the total saturated hydraulic conductivity (i.e., including both micropores and macropores) was set to 20 mm h^{-1}, and the kinematic exponent was set to 2. The model was run for two different values of the diffusion path length to simulate intermediate (d = 60 mm) and slow (d = 300 mm) exchange of energy between domains (Eq. [11]).

For this test case, in addition to the previously described measures taken to limit numerical artifacts (see above), we allowed oversaturation in the micropore domain when solving Richards' equation. Any water in excess of θ_b was then redistributed to the numerical layer above, and pressure potentials were updated accordingly. Finally, to smooth out the large gradients in pressure potential at the freezing front, gradients were estimated across a distance equal to three times the numerical layer thickness (i.e., the gradient between layer i and layer i + 1 was estimated from the pressure potentials in layer i − 1 and layer i + 2). This "smoothing" of gradients in pressure potentials was introduced to limit water flow at the thawing front and thereby stabilize the numerical solution to Richards' equation. In the original MACRO model, gradients are estimated between adjacent numerical layers. We used a simulation time step of 1 s, which resulted in run times of about 3 min on a standard laptop computer for a 120-h simulation.

Results and Discussion

Redistribution of Water in the Micropore Domain during Freezing (Test Case 1)

As soil water freezes from the soil surface, the pressure potential decreases and creates a hydraulic gradient directed toward the frozen part of the soil. This gradient creates an upward flow of water, which leads to increased water content close to the surface (Fig. 3). The model simulated this process well, with the depth of the freezing front (i.e., where there is a large decrease in water contents with increasing depth) accurately reproduced, especially at 24 and 50 h. Differences between measurements and modeling results are possibly due to uncertain estimates of the boundary heat flow and hydraulic conductivity, as discussed by Hansson et al. (2004). The small differences between the simulation results for the MACRO model and the model by Dall'Amico et al. (2011) are probably due to differences in spatial and temporal discretization.

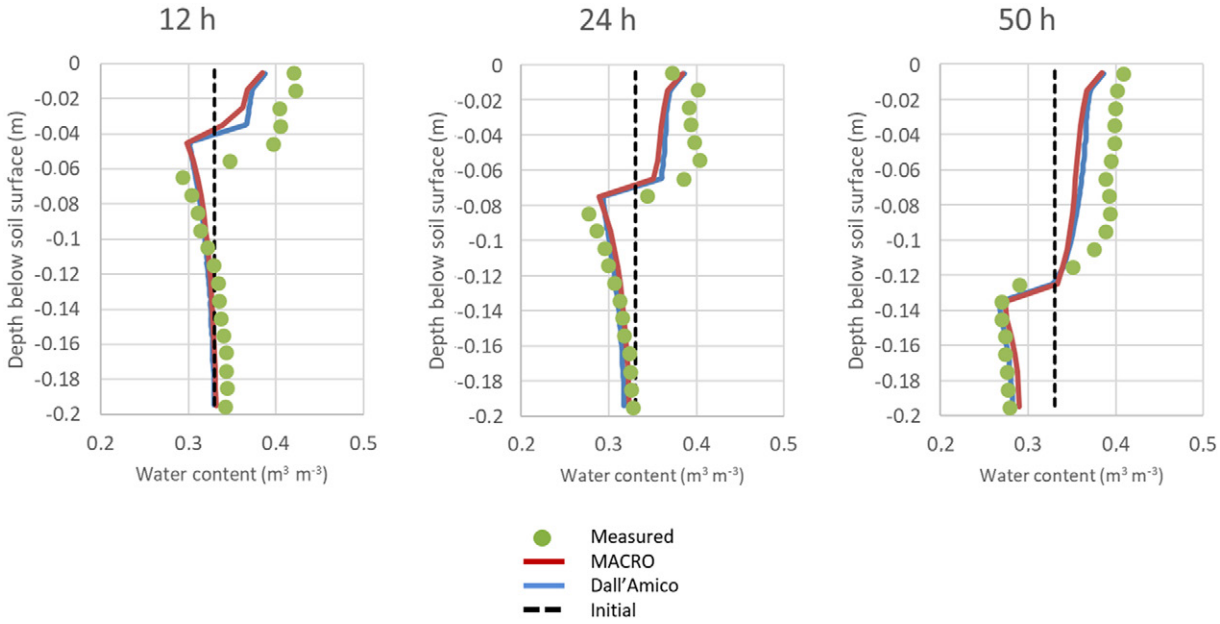

Fig. 3. Measured (Mizoguchi, 1990) and modeled (MACRO) distribution of water (liquid and ice) in the soil micropore domain during freezing from the soil surface (Test Case 1) at three time points. Modeling results from Dall'Amico et al. (2011) are included for comparison.

Comparison between First-Order Energy Transfer and the Heat Flow Equation (Test Case 2)

For the simulations without freezing, the FOET approach reproduced the energy exchange and the average temperature given by the heat conduction equation well (Fig. 4a and 4b). The FOET was smaller than the mean energy transfer from the heat flow equation simulations during the initial phase, which resulted in an underestimation of the average temperature. Because the temperature close to the macropore wall (x = 0 cm), which determines the driving force for energy transfer for the heat flow equation, increases much faster than the micropore domain temperature for the FOET approach, the energy exchange also decreases faster.

For the simulations accounting for freezing, both the energy exchange and the average temperature were less accurately reproduced by the FOET approach (Fig. 4c and 4d). The gradual increase in average temperatures during the thawing process simulated by the heat flow equation cannot be captured by the FOET approach because the temperature in the soil matrix is represented by only one value and all soil water thaws at temperatures close to 0°C. Even though the energy needed to melt the ice is equal for the two approaches, the time needed for complete melting differed. It took longer to completely thaw the soil for the FOET approach (about 20 h) than the heat flow equation (about 15 h). The changes in the total energy content of the soil matrix is determined by the energy flux at the boundary between the pore domains. When soil freezing is accounted for, larger temperature gradients are maintained at the boundary, which leads to larger energy fluxes. This effect is larger for the simulations with the heat flow equation compared with the FOET approach. The much larger initial energy exchange for the simulations accounting for freezing (Fig. 4a and 4c) is due to the larger thermal conductivity of ice (2.2 W m^{-1} $°C^{-1}$) than liquid water (0.57 W m^{-1} $°C^{-1}$).

The FOET model is an approximation of the heat flow equation and a perfect fit should, therefore, not be expected. Although it would be interesting, we did not investigate the possible consequences of the difficulties in simulating energy transfer between pore domains during thawing for the different modeling scenarios.

Water Flow in Macropores during Freezing (Test Case 3)

The simulation results without freezing show a kinematic wave moving down through the soil macropores (dotted line in Fig. 5). The velocity of the wave decreases on cessation of irrigation as the degree of saturation in the wave decreases (Eq. [1]). Before the start of the third irrigation, the wave from the second irrigation has intercepted the first wave (Fig. 5d). At the end of the simulation, the infiltrated water has reached a depth of 12 cm (Fig. 5f).

The patterns of simulated water contents were very different when freezing was accounted for, especially toward the end of the simulation. Freezing started immediately when water infiltrated into the macropores (Fig. 5a and 5b). Before the onset of the second irrigation, all water in the surface 1.5 cm was frozen (Fig. 5c). At this time, water existed both in liquid form and as ice below the 1.5-cm depth. With consecutive irrigations, a larger fraction of the macroporosity became blocked with ice. At the end of the simulation, the macropores were completely blocked by ice at the soil surface, which prevented further infiltration (Fig. 5f).

Simulation results are in line with the current perception of the processes and the limited data on water flow through macropores (Watanabe and Kugisaki, 2017). However, the model should now be evaluated and tested against measured data on the

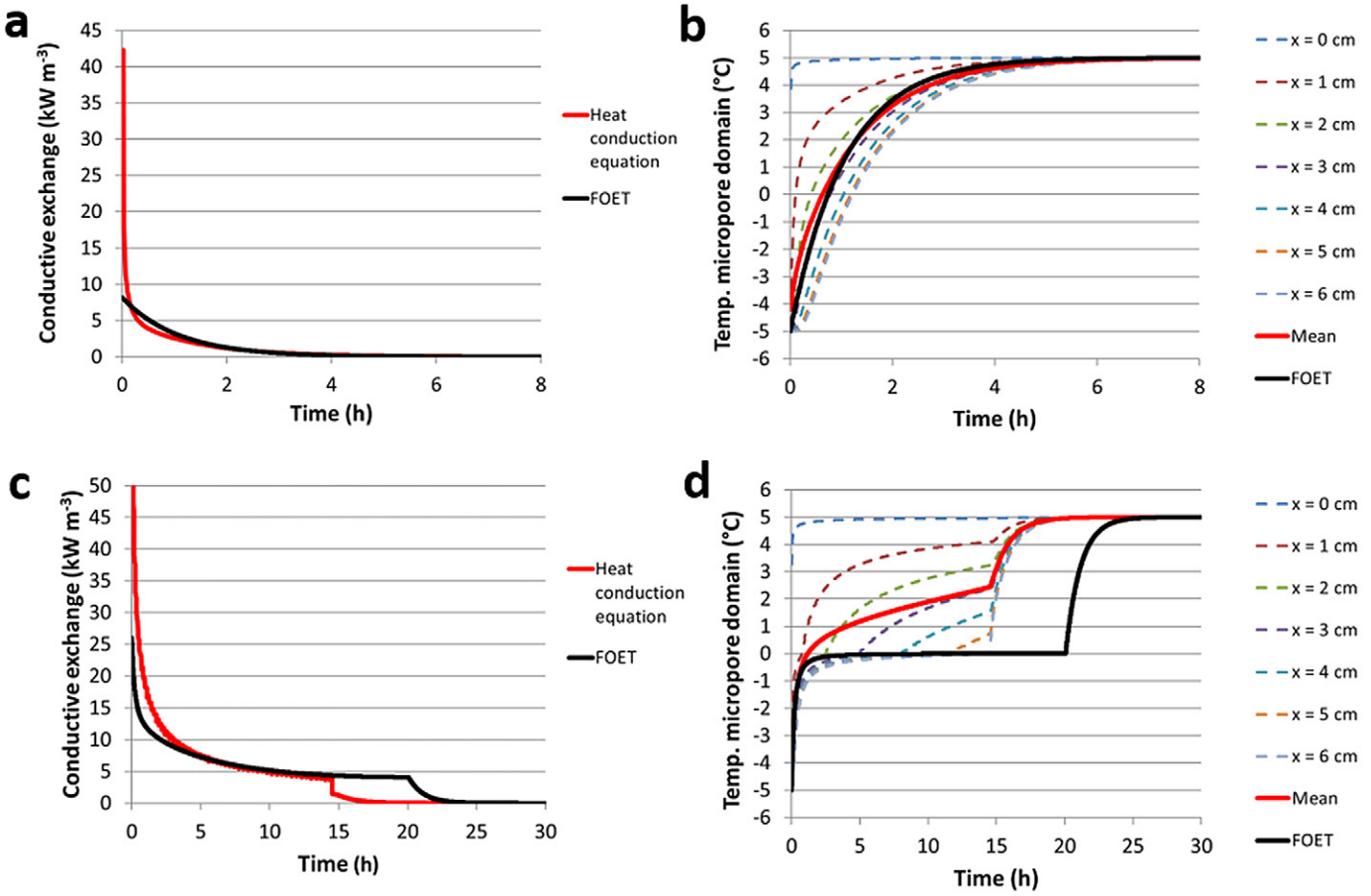

Fig. 4. Comparison between first-order energy transfer (FOET) and a numerical solution to the heat conduction equation (Test Case 2) (a,b) without freezing and (c,d) with freezing, showing (a,c) the energy exchange from the macropore domain to the micropore domain and (b,d) temperatures in the micropore domain. The solution to the heat flow equation is given for different distances (x) from the boundary and as the mean value. The vertical axis in (c) was adjusted for improved resolution. The conductive exchange for the heat conduction equation at t = 0 h was 290 kW m^{-3}. Note the different scales on horizontal and vertical axes.

distribution of ice in macropore networks following infiltration into frozen soil for soils with contrasting macropore structure, initial conditions, and boundary conditions. Such data could be provided through X-ray imaging of frozen macroporous soils before and after infiltration events.

Thawing of Initially Frozen Soil during Constant Rainfall (Test Case 4)

The pattern of simulated soil temperatures is similar to those observed in experimental studies with similar boundary conditions (Holten et al., 2018). Soil temperatures close to the surface increase very quickly toward the air temperature (Fig. 6a and 6b). With increasing depth, a more pronounced plateau at temperatures just below 0°C develops. In this temperature range, the energy supplied from the soil surface is used for the phase change from ice to liquid water rather than to increase temperatures.

The freezing and melting of water in the macropores is governed by the transfer of energy between pore domains (Eq. [11]). To illustrate this process, the conductive energy transfer, EX_{cond}, at the 10-cm depth is shown as an example in Fig. 6c and 6d. During the initial phase, the infiltration capacity of the frozen matrix is limited and water at an initial temperature of 7°C enters the macropore domain. This results in an energy transfer from the macropore domain to the initially frozen micropore domain. Temperatures in the macropore domain decrease and freezing starts if temperatures reach 0°C. Figures 6e and 6f show the degree of ice saturation in the macropores, $S_{ice} = \theta_{mac,ice}/\varepsilon_{mac,tot}$, where a value of 1 means that the macropore domain is completely blocked by ice. For the simulations with intermediate transfer, the negative energy transfer at the 10-cm depth stops after a few hours (Fig. 6c) when the macropore domain becomes completely blocked by ice down to a depth of 10 cm (Fig. 6e) and temperatures in the two domains reach equilibrium. When the temperature in the micropore domain increases due to thawing from the top (Fig. 6a), energy transfer from the micropore domain to the completely frozen macropore domain starts and the ice in the macropore domain starts to melt when temperatures reach 0°C. For the intermediate energy transfer simulations, this happens for the 10-cm depth at about t = 27 h (Fig. 6c). When all ice in the macropore domain has melted (t = 38 h), temperatures in the pore domains again reach equilibrium. For the slow energy transfer simulation, the macropore domain never gets completely blocked by ice, and

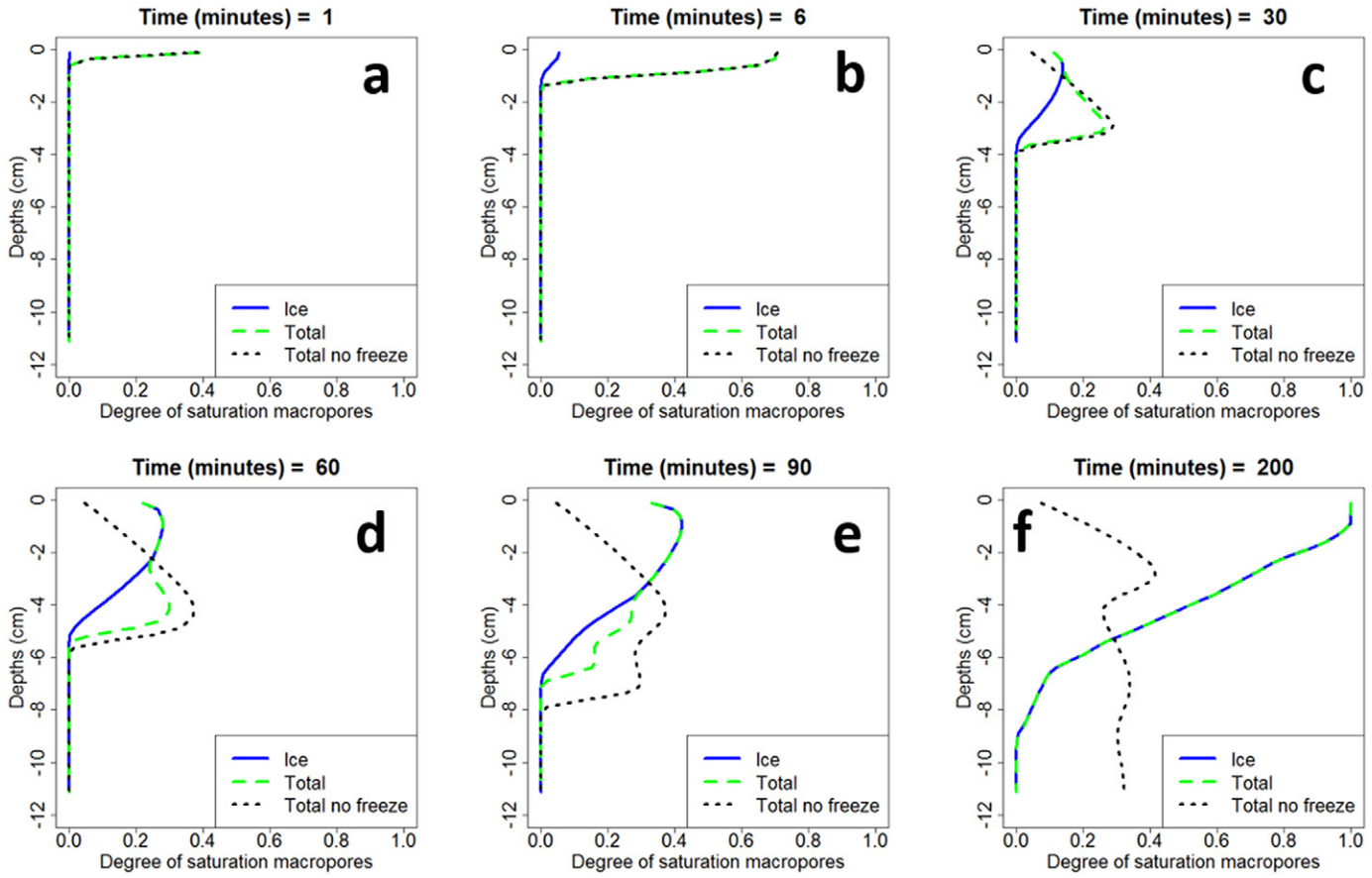

Fig. 5. Simulation results for macropore infiltration (Test Case 3) with and without freezing with (a) initially air-filled macropores, (b) after Irrigation 1, before Irrigations (c) 2, (d) 3, and (e) 4, and (f) final state.

the energy transfer from the macropore domain to the micropore domain continues until the micropore domain is completely thawed at the 10-cm depth at about $t = 26$ h (Fig. 6b, 6d, and 6f). At $t > 26$ h, energy is transferred from the micropore domain to the partly frozen macropore domain (Fig. 6d and 6f).

Water flow in the macropores starts as soon as there is some liquid water in the macropores (Eq. [1] and [10]). As water in the macropores moves downward, it may again reach depths where the soil is frozen and the water refreezes due to energy transfer from the macropore to the micropore domain. This process can be seen in the increase in the degree of ice saturation at the 15-cm depth at $t = 45$ h and at the 20-cm depth at about $t = 68$ h (Fig. 6e).

The total percolation at the bottom of the column is dominated by percolation from the macropores until the soil is completely melted because the hydraulic conductivity of the micropores is severely reduced by ice (Fig. 6g and 6h). The percolation for the simulations with intermediate energy transfer shows an initial peak where percolation equals the rain intensity of 1.5 mm h^{-1} (Fig. 6g). The rain infiltrates into the initially air-filled macropores, and water continues to flow until ice completely blocks the macropore domain, when percolation drops to zero. Percolation starts again when ice no longer completely blocks the macropore domain at any depth. At $t = 80$ h, the micropore domain is completely thawed (Fig. 6a) and no more refreezing of macropore water occurs. Water stored in the macropore domain above previously frozen layers can now flow unhindered and the percolation reaches a peak value of almost 5 mm h^{-1}. Finally, percolation recedes to the rainfall intensity of 1.5 mm h^{-1}. The results from the simulations with slow and intermediate energy transfer between pore domains are in line with dye tracer experiments conducted under winter conditions, which show that, depending on boundary conditions and soil properties, snowmelt infiltration may either be blocked by ice or bypass frozen layers through initially air-filled macropores (Stähli et al., 2004; Demand et al., 2019).

For the slow transfer rate simulations, infiltration equals the rainfall intensity throughout the simulation because the macropore domain never becomes completely blocked by ice (Fig. 6d and 6h). Hence the infiltrating water continuously adds energy to the soil. This is not the case for the intermediate transfer rate simulations, where infiltration is limited for a large part of the simulation due to ice blocking both pore domains. Despite an intermediate transfer rate of energy, the total cumulative energy transfer for the whole column was, for this simulation, smaller than for the slow transfer (not shown). These differences in total cumulative energy transfer between simulations resulted in differences in the time needed to completely thaw the 20-cm soil column (80 and 73 h for the intermediate and slow transfer rates, respectively).

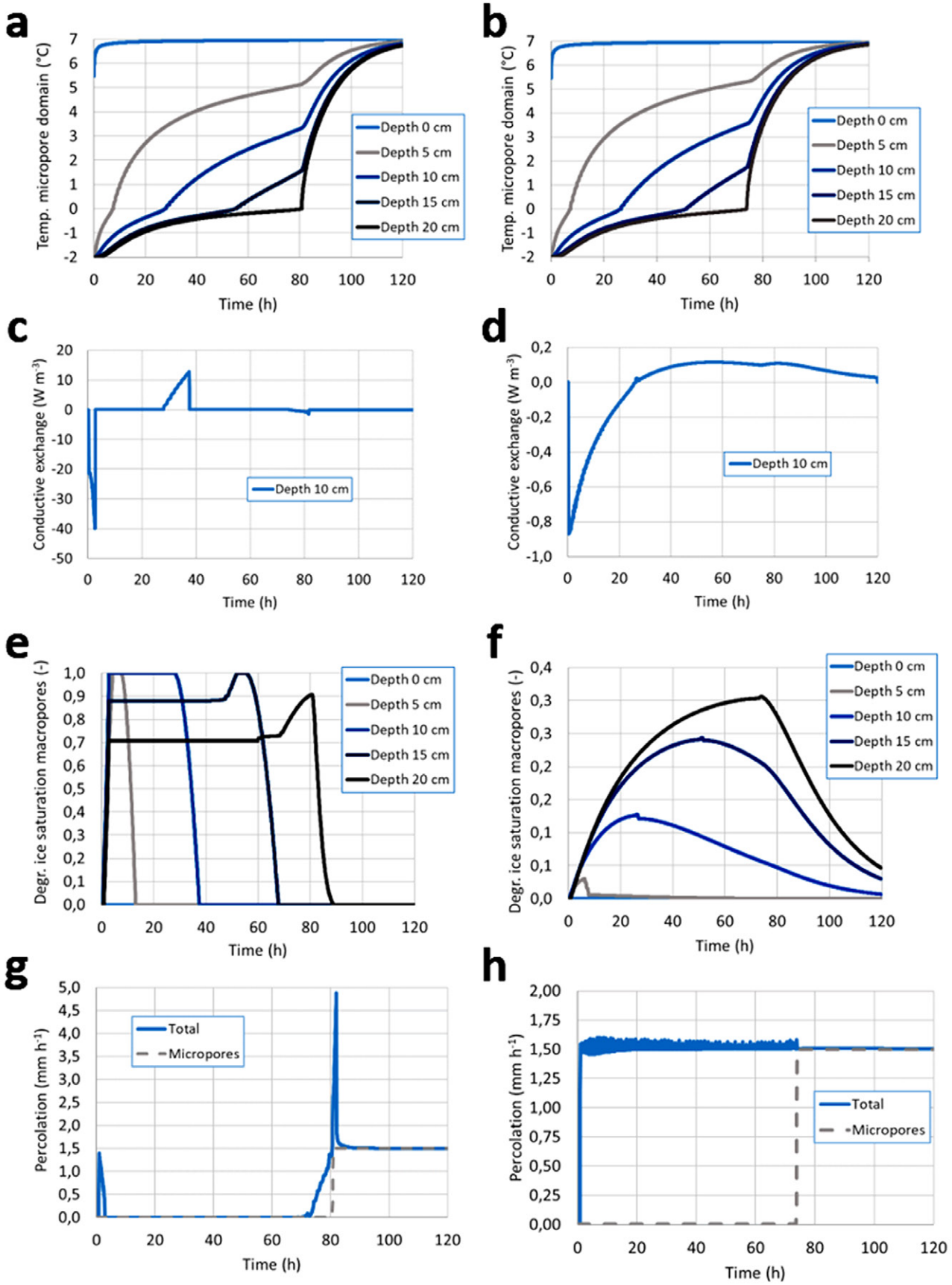

Fig. 6. Simulation results for thawing during constant rainfall (Test Case 4) for simulations with (a,c,e,g) intermediate (d = 60 mm) and (b,d,f,h) slow (d = 300 mm) energy transfer between pore domains: (a,b) soil temperatures at five depths below the soil surface; (c,d) conductive energy transfer at the 10-cm depth; (e,f) the degree of ice saturation in the macropores; and (g,h) percolation at the bottom of the soil column. Note the different scales on the vertical axes.

Despite the measures taken to limit numerical artifacts (see above), the percolation for the slow transfer simulations shows fluctuations until the micropore domain was completely thawed (Fig. 6h). These artifacts do call for further investigation. However, they did not influence the interpretation of the results and did not cause errors in the water balance (relative error <0.0001%).

Conclusions

We have presented a first attempt to include the effects of soil freezing in a physically based dual-permeability model for water flow and heat transport. The model enables the simulation of preferential water flow through frozen soil with initially air-filled macropores, a situation that is often encountered during snowmelt. Results from the four test cases investigated here show that the model reproduces the limited available measured data well and that it behaves in accordance with the current understanding of water flow and heat transport in macroporous soil. We acknowledge that measured data for a quantitative model evaluation is largely lacking. To improve modeling of water and heat flow in frozen soils further, attention should be focused on providing experimental data suitable for evaluating models accounting for macropore flow.

Acknowledgments

This study was funded by the Research Council of Norway (Smartcrop, Project no. 244526/E50) and the Center for Chemical Pesticides at the Swedish University of Agricultural Sciences (SLU).

References

Beven, K., and P. Germann. 1982. Macropores and water flow in soils. Water Resour. Res. 18:1311–1325. doi:10.1029/WR018i005p01311

Campbell, G.S. 1985. Soil physics with Basic: Transport models for soil–plant systems. Elsevier, New York.

Dall'Amico, M., S. Endrizzi, S. Gruber, and R. Rigon. 2011. A robust and energy-conserving model of freezing variably-saturated soil. Cryosphere 5:469–484. doi:10.5194/tc-5-469-2011

Demand, D., J. Selker, and M. Weiler. 2019. Influences of macropores on infiltration into seasonally frozen soil. Vadose Zone J. 18:180147. doi:10.2136/vzj2018.08.0147

FOCUS Working Group on Surface Water Scenarios. 2001. Forum for the coordination of pesticide fate models and their use. FOCUS surface water scenarios in the EU evaluation process under 91/414/EEC. EC Doc. Ref. Sanco/4802/2001-rev.1.221. EU Commission, Brussels.

Gerke, H.H., and M.Th. van Genuchten. 1993. Evaluation of a first-order water transfer term for variably saturated dual-porosity flow models. Water Resour. Res. 29:1225–1238. doi:10.1029/92WR02467

Gerke, H.H., and M.Th. van Genuchten. 1996. Macroscopic representation of structural geometry for simulating water and solute movement in dual-porosity media. Adv. Water Resour. 19:343–357. doi:10.1016/0309-1708(96)00012-7

Hansson, K., J. Šimůnek, M. Mizoguchi, L.-C. Lundin, and M.Th. van Genuchten. 2004. Water flow and heat transport in frozen soil. Vadose Zone J. 3:693–704. doi:10.2136/vzj2004.0693

Holten, R., F.N. Bøe, M. Almvik, S. Katuwal, M. Stenrød, M. Larsbo, et al. 2018. The effect of freezing and thawing on water flow and MCPA leaching in partially frozen soil. J. Contam. Hydrol. 219:72–85. doi:10.1016/j.jconhyd.2018.11.003

Ireson, A.M., G. van der Kamp, G. Ferguson, U. Nachshon, and H.S. Wheater. 2013. Hydrogeological processes in seasonally frozen northern latitudes: Understanding, gaps and challenges. Hydrogeol. J. 21:53–66. doi:10.1007/s10040-012-0916-5

Jansson, P.-E. 2012. CoupModel: Model use, calibration, and validation. Trans. ASABE 55:1337–1346. doi:10.13031/2013.42245

Jarvis, N. 1994. The MACRO model (Version 4.2). Technical description. Rep. and Diss. 19. Dep. of Soil Sci., Swedish Univ. of Agric. Sciences, Uppsala.

Jarvis, N.J. 2007. A review of non-equilibrium water flow and solute transport in soil macropores: Principles, controlling factors and consequences for water quality. Eur. J. Soil Sci. 58:523–546. doi:10.1111/j.1365-2389.2007.00915.x

Jarvis, N.J., P.-E. Jansson, P.E. Dik, and I. Messing. 1991. Modeling water and solute transport in macroporous soil: 1. Model description and sensitivity analysis. J. Soil Sci. 42:59–70. doi:10.1111/j.1365-2389.1991.tb00091.x

Jarvis, N., J. Koestel, and M. Larsbo. 2016. Understanding preferential flow in the vadose zone: Recent advances and future prospects. Vadose Zone J. 15(12). doi:10.2136/vzj2016.09.0075

Jarvis, N., and M. Larsbo. 2012. MACRO (v5.2): Model use, calibration, and validation. Trans. ASABE 55:1413–1423. doi:10.13031/2013.42251

Jones, J.A.A. 2010. Soil piping and catchment response. Hydrol. Processes 24:1548–1566. doi:10.1002/hyp.7634

Kane, D.L. 1980. Snowmelt infiltration into seasonally frozen soils. Cold Reg. Sci. Technol. 3:153–161. doi:10.1016/0165-232X(80)90020-8

Kelleners, T.J. 2013. Coupled water flow and heat transport in seasonally frozen soils with snow accumulation. Vadose Zone J. 12(4). doi:10.2136/vzj2012.0162

Koopmans, R.W.R., and R.D. Miller. 1966. Soil freezing and soil water characteristic curves. Soil Sci. Soc. Am. J. 30:680–685. doi:10.2136/sssaj1966.03615995003000060011x

Kurylyk, B.L., and K. Watanabe. 2013. The mathematical representation of freezing and thawing processes in variably-saturated, non-deformable soils. Adv. Water Resour. 60:160–177. doi:10.1016/j.advwatres.2013.07.016

Larsbo, M., S. Roulier, F. Stenemo, R. Kasteel, and N. Jarvis. 2005. An improved dual-permeability model of water flow and solute transport in the vadose zone. Vadose Zone J. 4:398–406. doi:10.2136/vzj2004.0137

Lundberg, A., P. Ala-Aho, O.M. Eklo, B. Klöve, J. Kværner, and C. Stumpp. 2016. Snow and frost: Implications for spatiotemporal infiltration patterns: A review. Hydrol. Processes 30:1230–1250. doi:10.1002/hyp.10703

Lundin, L.-C. 1990. Hydraulic properties in an operational model of frozen soil. J. Hydrol. 118:289–310. doi:10.1016/0022-1694(90)90264-X

Mizoguchi, M. 1990. Water, heat and salt transport in freezing soil. (In Japanese.) Ph.D. diss. Univ. of Tokyo.

Mohammed, A.A., B.L. Kurylyk, E.E. Cey, and M. Hayashi. 2018. Snowmelt infiltration and macropore flow in frozen soils: Overview, knowledge gaps, and a conceptual framework. Vadose Zone J. 17:180084. doi:10.2136/vzj2018.04.0084

Mualem, Y. 1976. A new model for predicting the hydraulic conductivity of unsaturated porous media. Water Resour. Res. 12:513–522. doi:10.1029/WR012i003p00513

R Core Team. 2018. R: A language and environment for statistical computing. R Found. Stat. Comput., Vienna.

Seyfried, M.S., and M.D. Murdock. 1997. Use of air permeability to estimate infiltrability of frozen soil. J. Hydrol. 202:95–107. doi:10.1016/S0022-1694(97)00061-9

Šimůnek, J., M.Th. van Genuchten, and M. Šejna. 2016. Recent developments and applications of the HYDRUS computer software packages. Vadose Zone J. 15(7). doi:10.2136/vzj2016.04.0033

Stadler, D., M. Stähli, P. Aeby, and H. Flühler. 2000. Dye tracing and image analysis for quantifying water infiltration into frozen soils. Soil Sci. Soc. Am. J. 64:505–516. doi:10.2136/sssaj2000.642505x

Stähli, M., D. Bayard, H. Wydler, and H. Flühler. 2004. Snowmelt infiltration into alpine soils visualized by dye tracer technique. Arct. Antarct. Alp. Res. 36:128–135. doi:10.1657/1523-0430(2004)036[0128:SIIASV]2.0.CO;2

Stähli, M., P.-E. Jansson, and L.-C. Lundin. 1996. Preferential water flow in a frozen soil: A two-domain model approach. Hydrol. Processes 10:1305–1316. doi:10.1002/(SICI)1099-1085(199610)10:10<1305::AID-HYP462>3.0.CO;2-F

Stähli, M., P.-E. Jansson, and L.-C. Lundin. 1999. Soil moisture redistribution and infiltration in frozen sandy soils. Water Resour. Res. 35:95–103. doi:10.1029/1998WR900045

van der Kamp, G., M. Hayashi, and D. Gallén. 2003. Comparing the hydrology of grassed and cultivated catchments in the semi-arid Canadian prairies. Hydrol. Processes 17:559–575. doi:10.1002/hyp.1157

van Genuchten, M.Th. 1980. A closed-form equation for predicting the hydraulic conductivity of unsaturated soils. Soil Sci. Soc. Am. J. 44:892–898. doi:10.2136/sssaj1980.03615995004400050002x

Watanabe, K., and Y. Kugisaki. 2017. Effect of macropores on soil freezing and thawing with infiltration. Hydrol. Processes 31:270–278. doi:10.1002/hyp.10939

Williams, P.J., and M.W. Smith. 1989. The frozen earth: Fundamentals of geocryology. Cambridge Univ. Press, Cambridge, UK. doi:10.1017/CBO9780511564437